Postinspiratory activity of costal and crural diaphragm

P. A. EASTON, M. KATAGIRI, T. M. KIESER, AND R. S. PLATT
Division of Critical Care, Department of Medicine, University of Calgary, Calgary, Alberta, Canada T2N 4N1

Easton, P. A., M. Katagiri, T. M. Kieser, and R. S. Platt. Postinspiratory activity of costal and crural diaphragm. *J. Appl. Physiol.* 87(2): 582–589, 1999.—Because the first stage of expiration or "postinspiration" is an active neurorespiratory event, we expect some persistence of diaphragm electromyogram (EMG) after the cessation of inspiratory airflow, as postinspiratory inspiratory activity (PIIA). The costal and crural segments of the mammalian diaphragm have different mechanical and proprioceptive characteristics, so postinspiratory activity of these two portions may be different. In six canines, we implanted chronically EMG electrodes and sonomicrometer transducers and then sampled EMG activity and length of costal and crural diaphragm segments at 4 kHz, 10.2 days after implantation during wakeful, resting breathing. Costal and crural EMG were reviewed on-screen, and duration of PIIA was calculated for each breath. Crural PIIA was present in nearly every breath, with mean duration 16% of expiratory time, compared with costal PIIA with duration −2.6% of expiratory time ($P < 0.002$). A linear regression model of crural centroid frequency vs. length, which was computed during the active shortening of inspiration, did not accurately predict crural EMG centroid frequency values at equivalent length during the controlled relaxation of postinspiration. This difference in activation of crural diaphragm in inspiration and postinspiration is consistent with a different pattern of motor unit recruitment during PIIA.

sonomicrometer; electromyogram; electromyogram spectrum; centroid frequency; postinspiratory inspiratory activity

EVEN LARGE MAMMALS seem to adhere to a three-phase model of respiration, where the first stage of expiration or "postinspiration" is an active neurorespiratory event (2, 3, 23). We expect some persistence of the diaphragm electromyogram (EMG) after the cessation of inspiratory airflow, usually titled postinspiratory inspiratory activity (PIIA). When concurrent measurements of diaphragm length are available, each breath presents as a period of active shortening followed by active, controlled relaxation, because postinspiratory diaphragm lengthening occurs while EMG PIIA persists (8).

Because the costal and crural segments of the mammalian diaphragm are distinct, postinspiratory activity of these two portions may also be different. Certainly, the proprioceptive characteristics of costal and crural are different, as expressed by muscle spindle content (6, 18), suggesting that the segments are not equally suited for a controlled relaxation or "braking" action (22). Although there has been some evidence in awake mammals that resting costal and crural postinspiratory activity is similar (27), we reported significant differences in PIIA during resting, hypercapnic, and hypoxic breathing in the awake canine (7–9). However, our prior studies were not designed specifically to study PIIA. In those earlier reports we relied exclusively on tracheotomized animals, recorded EMG only as a moving average with a moderate time constant, and depended on a normalized bin analysis to compare PIIA timing between the segments. Therefore, in this study, in a group of chronically implanted, awake canines, with intact upper airways, we recorded costal and crural EMG at rates of sampling, which provided a high-resolution comparison of the postinspiratory activity of the two diaphragm segments.

We are unaware of any existing information about the EMG spectrum during postinspiration, except for the historic observation that there is a brief, visible interruption in the inspiratory EMG, at the instant postinspiratory activity begins, and that the decrescendo EMG that follows in postinspiration is distinct from the activity in inspiration (4, 24). Classically, this has been cited as evidence that postinspiratory activity is not a simple decay of inspiratory activity (4), but there has not been any quantitative comparison of inspiration and postinspiration EMG. Intuitively, recruitment patterns of motor units would be expected to change during "braking"; at the least, firing rates of motor units active during inspiration should slow. Therefore, during PIIA compared with inspiration, we would expect a shift to lower values of a measure of central tendency of the power spectrum such the centroid frequency (Fc), but this has not been tested. To be valid, any comparison of EMG spectrum between inspiration and postinspiration requires that there cannot be any changes in muscle and electrode geometry that could confound the results. Because our canines provide continuous direct measurements of contraction and then relaxation of diaphragm length throughout each breath, we were able to compare the EMG spectrum of inspiration and postinspiration at equivalent muscle lengths.

METHODS

Surgical implantation. The project was approved by the animal care committee at the University of Calgary. Each mongrel canine had pairs of bipolar fine-wire EMG electrodes and sonomicrometry transducers implanted in left costal and crural diaphragm segments. This technique of chronic sonomicrometry and EMG implantation, and the 7- to 10-day progressive recovery of diaphragm segmental shortening, has been described in detail elsewhere (8, 14). Briefly, while the canines were under general anesthesia, the left hemidiaphragm was exposed through a midabdominal incision, and ultrasonic transducers were implanted between muscle fibers on the lateral portion of the costal segment corresponding

The costs of publication of this article were defrayed in part by the payment of page charges. The article must therefore be hereby marked "*advertisement*" in accordance with 18 U.S.C. Section 1734 solely to indicate this fact.

roughly to the second sternocostal branch of the phrenic nerve (12), approximately midway between central tendon and chest wall, and in the posterior, perivertebral region of the crural segment. On each segment immediately adjacent to each pair of transducers, a fine-wire stainless steel bipolar EMG electrode was attached. All implants were secured by fine, synthetic, nonfibrogenic sutures (Prolene, Ethicon), wires were externalized, and the animals were recovered.

Measurement techniques. All measurements of ventilation and respiratory muscle function were performed with the animals awake and breathing quietly, while lying in the right lateral decubitus position, which placed the implanted hemidiaphragm in a nondependent position. The animals were familiar with the location, routine, and personnel of the recordings. The animals breathed spontaneously through a snout mask, which was connected through a one-way valve to a low-resistance open-breathing circuit (<1 $cmH_2O \cdot l^{-1} \cdot s$), which incorporated a pneumotachograph (Fleisch no. 2) and a piezoelectric differential-pressure transducer (model 163PC01D36, Honeywell Microswitch) connected across the pneumotachograph to provide measurement of inspiratory airflow. Dynamic measurement within the respiratory muscles, of the changing distance between the sonomicrometer transducers of each pair, was provided by measuring the speed of transmission of ultrasonic waves by using a sonomicrometer (model 120, Triton Technology, San Diego, CA) (8). The output signal of the sonomicrometer was offset, amplified, and then sampled to computer.

With use of computer software for data acquisition (DataSponge, Bioscience Analysis Software, Calgary, AB), all signals were monitored in real time on the computer display and simultaneously collected to hard disk on a microcomputer (IBM, White Plains, NY) equipped with a single-board analog-to-digital system (model MIO-16-H-9, National Instruments, Galveston, TX). Inspiratory airflow and costal and crural length and EMG were recorded continuously to the disk at sampling rates of 100 Hz; all EMG signals and electrocardiogram were sampled at 4 kHz.

For measurement of EMG, the fine-wire bipolar electrode pair was connected to an alternating-current differential preamplifier (model 1700, AM Systems, Everett, WA). Power line interference was abolished by careful shielding techniques and the use of differential preamplifiers with a high common-mode signal rejection of 110 dB. Thereafter, the signal was filtered to attenuate movement artifact and sonomicrometry noise and perform antialias filtering, by using a six-pole, low-pass Bessel filter at 700 Hz (model 746, LT-4, Frequency Devices, Haverhill, MA) and a matching, six-pole, high-pass filter at 20 Hz. The EMG signals were further amplified before being sampled by computer at 4 kHz. Electrocardiogram was obtained concurrently. A representative trace of airflow, costal and crural length, and raw EMG are shown in Fig. 1.

Analysis of ventilation, shortening, and duration of postinspiratory EMG. The flow signal was evaluated for respiratory timing by using our analysis software programs and was digitally integrated; inspiratory time, expiratory time (T_E), total breath time, respiratory frequency, tidal volume, and minute ventilation were calculated breath by breath. By using the recorded flow and length signals, the software identified the baseline, resting length of the inspiratory muscles at end expiration, and then shortening for each breath was expressed as a percent change from resting length entitled. These calculations have been described in detail elsewhere (8, 14). With use of our computer software (DataSponge), the raw traces of costal and crural EMG, which had been sampled at 4 kHz, were replayed on the computer screen. The exact moment where inspiratory EMG activity ceased for costal and crural segments for each breath, and its temporal relationship to inspiratory airflow, was visualized on-screen and marked digitally. Then the duration of EMG postinspiratory activity for each segment for each breath was

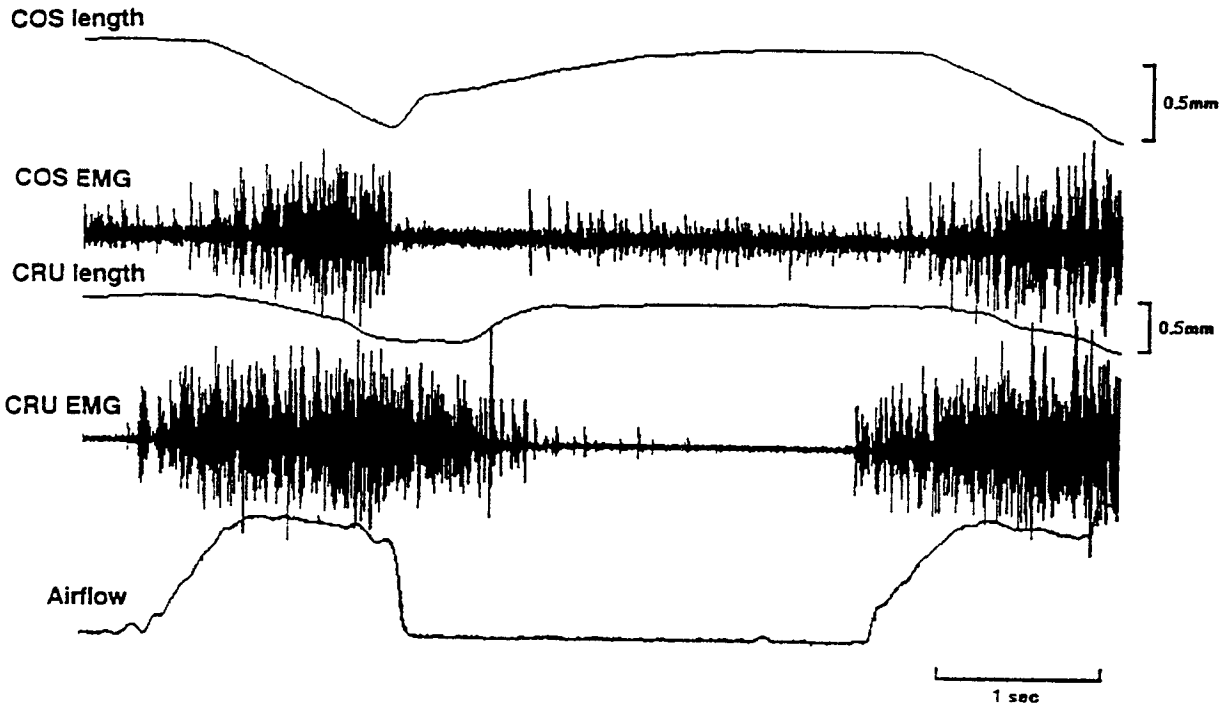

Fig. 1. Costal (COS) and crural (CRU) length, raw EMG, and airflow. From *top* to *bottom*, traces show COS diaphragm length and EMG, CRU length and EMG, and inspiratory airflow. Recordings are from chronically implanted electrodes in an individual awake canine subject. Postinspiratory inspiratory activity (PIIA) of crural EMG is prominent; costal PIIA EMG is absent.

calculated in milliseconds and expressed as a percentage of TE, for each breath.

EMG power spectral analysis. A second suite of dedicated computer analysis programs examined EMG power spectra. The first of these programs included precise, frequency-selective, finite-impulse-response digital filters (19). Sonomicrometer noise was removed with narrow-notch filters, and movement artifact was removed by using a very sharp, high-pass filter with a 25-Hz cutoff frequency. Filtered power spectra were inspected to verify that the filtering process was successful in removal of interference-noise spikes. The filtered EMG signals were then processed to obtain a running value of Fc (16), by selecting 128-point (32-ms) segments of EMG data and computing the power spectral density and Fc of each segment. Successive segments were selected by shifting sequentially 40 data points (10 ms) through the EMG data, which provided a continuous trace of EMG Fc with an effective sample rate of 100 Hz.

Once the raw EMG signals were preprocessed, the program suite proceeded with intrabreath EMG analysis. Beginning 1 s before the end of inspiratory airflow, to 1 s after the end of inspiratory airflow, sequential data epochs 10 ms apart were selected for analysis. Any of these data points that occurred in the vicinity of a cardiac QRS complex were omitted from analysis. At each sequential epoch position, a set of values, including EMG power, EMG Fc, muscle length, and time from the beginning inspiration, was recorded as a data set. For each canine, all such data were loaded into a spreadsheet (Microsoft Excel, Microsoft, Redmond, WA) for regression analysis.

To maintain an adequate signal-to-noise ratio (1), and avoid inclusion of Fc values calculated on noise rather than EMG, a threshold for minimum power was chosen where variance of the Fc increased dramatically or where the Fc was significantly skewed by ambient noise. Above the threshold, the power spectrum was dominated by the EMG but below the threshold the power spectrum consisted primarily of ambient noise, as seen in the Fc values for the diaphragm generated during portions of expiration (see Fig. 3). Fc points with EMG power lower than this minimum threshold were discarded.

A linear regression model of EMG Fc as a function of crural muscle length was computed, on the basis of data during latter inspiration, specifically from 900 to 200 ms before the end of inspiratory airflow. The *F* score of the linear regression for each canine was inspected and confirmed to be highly significant ($P < 0.01$) before the regression was used for any predictive function, as described in the next paragraph.

Then, the linear regressions relating crural muscle length and EMG Fc during inspiration for each animal were used to predict the EMG Fc for each sequential 10-ms data epoch during the postinspiratory period, on the basis of the muscle lengths at each point in postinspiration. Both the actual, calculated crural Fc values in postinspiration, as well as the Fc values predicted from crural length measured during postinspiration, were grouped into 100-ms bins, averaged, and plotted. This provided two Fc profiles for comparison during postinspiration: the profile of actual Fc values that had been calculated from raw EMG during postinspiration, and the profile of Fc values that were predicted to occur on the basis of the measured length of crural diaphragm at each moment of postinspiration.

Statistical analysis. Mean values were exported for review to spreadsheet software (Microsoft Excel, Microsoft), to graphic software to output the figures (CorelDraw, Corel, Ottawa, ON), and to the personal computer version of SAS (SAS version 6, SAS Institute, Cary, NC) for statistical analysis (25). Values for tidal breaths were averaged, and then the mean values for parameters of breathing pattern, shortening and duration of EMG PIIA were compared by Student's paired *t*-test. Over the time period from 0 to 200 ms within the postinspiratory period, the mean values of actual and predicted Fc were compared by using a *t*-test.

RESULTS

Breathing pattern and segmental shortening. We studied six canines of mean weight 31.3 kg. Measurements were made after the diaphragm was fully recovered (8), which was mean 10.2 days after chronic implantation (range 7–13 days). For the group, mean minute ventilation was 8.8 ± 1.4 (SD) l/min, respiratory frequency was 18.8 ± 2.8 breaths/min, tidal volume was 0.47 ± 0.05 liter, inspiratory time was 1.28 ± 0.18 s, and TE was 2.0 ± 0.32 s. The mean resting length at end expiration of the crural and costal segments was 14.8 ± 8.0 and 11.2 ± 5.0 mm, respectively. Mean tidal shortening of crural diaphragm was 5.7 ± 3.7% of baseline end-expiratory length; mean costal shortening per breath was 5.3 ± 4.8%.

Costal and crural postinspiratory activity. Crural EMG PIIA was a consistent finding in nearly every breath in all canines. By contrast, as seen in Fig. 1, costal EMG PIIA was either absent or very brief in all animals. Certainly, costal EMG PIIA was always significantly less than crural. The duration of costal and crural diaphragm PIIA for all six animals is summarized graphically in Fig. 2. In two animals only, there was measurable costal PIIA of 3–4%, which was significantly less than crural in those animals. In the other four animals, even though there was extensive crural PIIA, costal EMG activity ceased completely before the cessation of inspiratory airflow. Overall, the mean

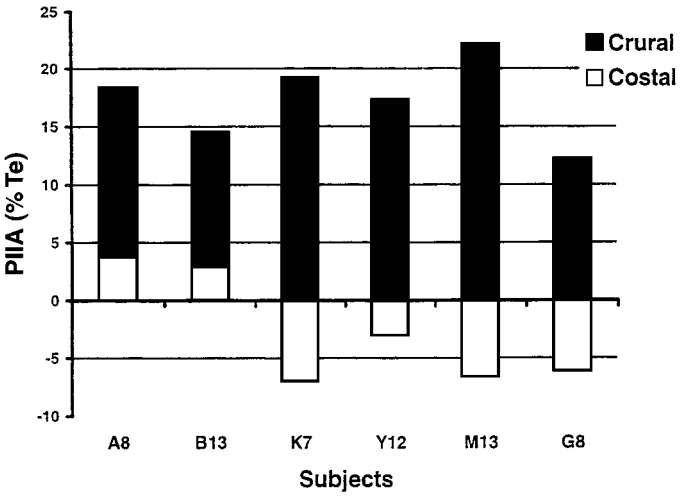

Fig. 2. Duration of costal and crural diaphragm EMG PIIA. *y*-Axis scale marks duration of PIIA as percent expiratory time (%TE). Individual canine subjects are listed along *x*-axis. Mean duration of PIIA for each subject is shown by histogram bars. Solid portion of each bar shows crural PIIA duration; open portion shows costal PIIA duration. Positive values of %TE indicate PIIA extending into expiration; negative values of PIIA indicate that EMG ceased before cessation of inspiratory airflow. In every subject, crural PIIA was significantly greater than costal PIIA.

duration of costal PIIA was −2.6% of TE; that is, average costal EMG typically stopped a few milliseconds before the end of inspiratory airflow. By contrast, mean crural PIIA persisted for the first 16% of TE into the subsequent expiration, which was significantly greater than costal ($P < 0.002$). Because costal PIIA was essentially absent, only crural PIIA was examined by spectral analysis, as described in the following two sections.

Crural EMG and Fc. An example of original crural length and raw EMG data, as well as derived values of EMG power and Fc, are illustrated for a single animal in Fig. 3. In this example, the momentary pause between inspiratory and postinspiratory activity of the EMG can be seen clearly in the raw EMG trace of the first breath. This type of brief cessation of EMG activity signifying the onset of PIIA was a very common observation among these canines. The termination of the postinspiratory activity of the crural EMG is also easily visible in the trace as well as the clear evidence from the power trace that the midexpiratory Fc values reflect only noise.

Baseline Fc values of crural diaphragm EMG were calculated, as well as the change in Fc over inspiratory time and the relationship of Fc to changing crural diaphragm length. For the group, the mean baseline Fc was 144 ± 49 (SD) Hz. Within a 700-ms period of inspiration, stretching from approximately −900 to −200 ms before the end of inspiratory airflow, the Fc increased at a mean rate of 17.1 ± 6.4 (SD) Hz/s. Finally, the linear regression analysis of crural Fc vs. crural diaphragm length performed on all data points over this same inspiratory period showed that the group mean Fc increased 7.3 ± 7.6 Hz per percent shortening of the diaphragm.

Crural postinspiratory EMG. All the Fc values throughout inspiration and postinspiration for a single animal are shown in Fig. 4. The horizontal axis marks the end of inspiration. Superimposed across this graph are the mean values of actual Fc per each 100-ms interval, as well as the corresponding values of Fc predicted over the same intervals. The predicted values of Fc were derived from the relationship between Fc and crural length, which was computed over the *left* half of the graph extending from −0.9 to −0.2 s, that is, during the time of inspiratory airflow. This "profile" of mean values per 100-ms interval was obtained by averaging bins of Fc values across each interval. As shown in Fig. 4, the actual and predicted profiles of Fc values diverged during postinspiration. The mean actual and predicted Fc values in the range of 0 to 200 ms after end inspiration were significantly different ($P < 0.001$). Thus the regression model that related crural length and Fc during inspiration did not successfully predict crural EMG Fc values during postinspiration. This significant discrepancy between Fc values of inspiration and postinspiration occurred for all six animals.

Figure 5 is a summary of the profiles of actual and predicted Fc for all animals. Because absolute Fc values varied among animals, the profiles were normalized to the predicted end-inspiration Fc value to allow

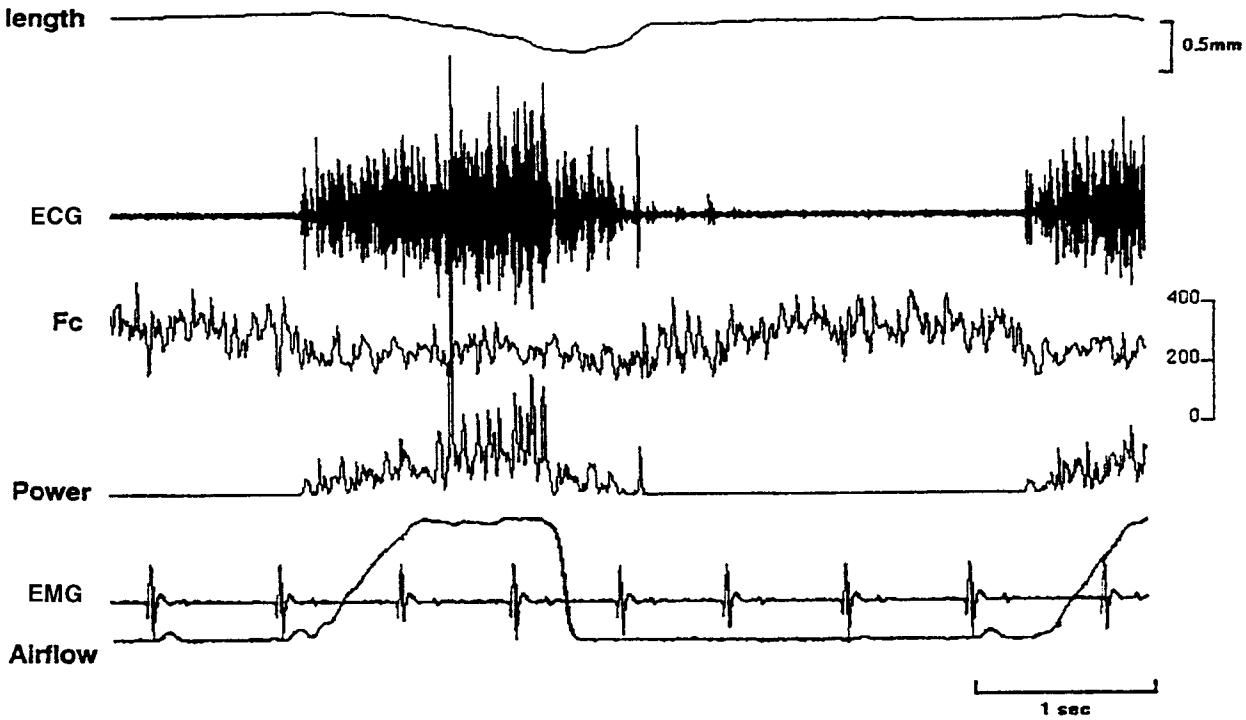

Fig. 3. Crural diaphragm length, raw EMG, centroid frequency (Fc), and power. *Top* 4 traces show crural diaphragm length and EMG, including raw EMG, crural spectral Fc, and EMG power. *Bottom* 2 traces show electrocardiogram (ECG) and inspiratory airflow. Spurious values of Fc are seen when there was very low EMG power. EMG calculations were performed only where there was sufficient EMG power and when ECG complexes were not present.

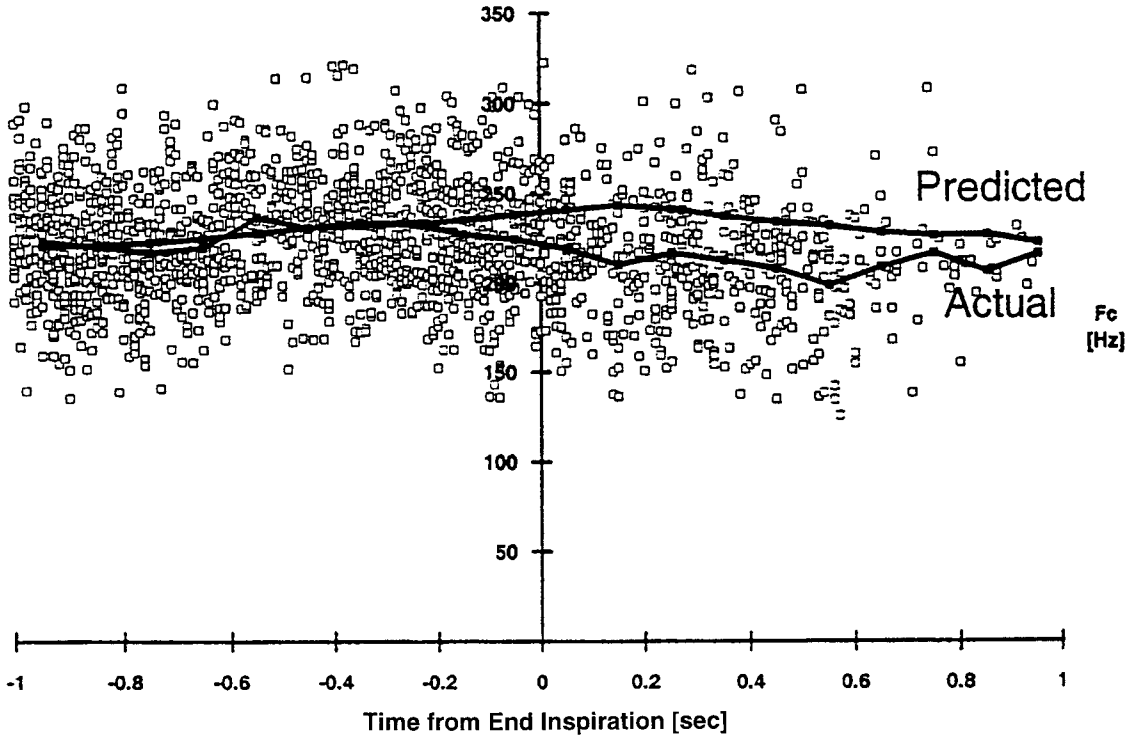

Fig. 4. Crural EMG Fc profile for a single subject. *y*-Axis shows Fc. *x*-Axis scale shows time from end inspiration. Positive times are postinspiratory, extending into subsequent expiration; negative times are during inspiration. All single Fc values calculated for this subject are shown by open squares. *Bottom* solid line and solid squares mark average actual Fc values over each 100-ms interval. *Top* solid line and solid squares mark average Fc value over each 100 ms, predicted from inspiratory relationship between length and Fc. During postinspiration, mean actual Fc values were significantly less than predicted.

comparison. Figure 5 illustrates that the relationship between crural diaphragm EMG Fc and crural length during inspiration was significantly different from postinspiration. During postinspiration, the Fc was at least 10% lower than expected, on the basis of equivalent length of the crural diaphragm during inspiration.

DISCUSSION

Crural prominence in PIIA. Crural PIIA was prominent in these animals, compared with costal PIIA. Either costal PIIA was absent altogether or it was minimal in duration compared with crural, which could be identified during most breaths and persisted on average for the first 16% of TE. These results were

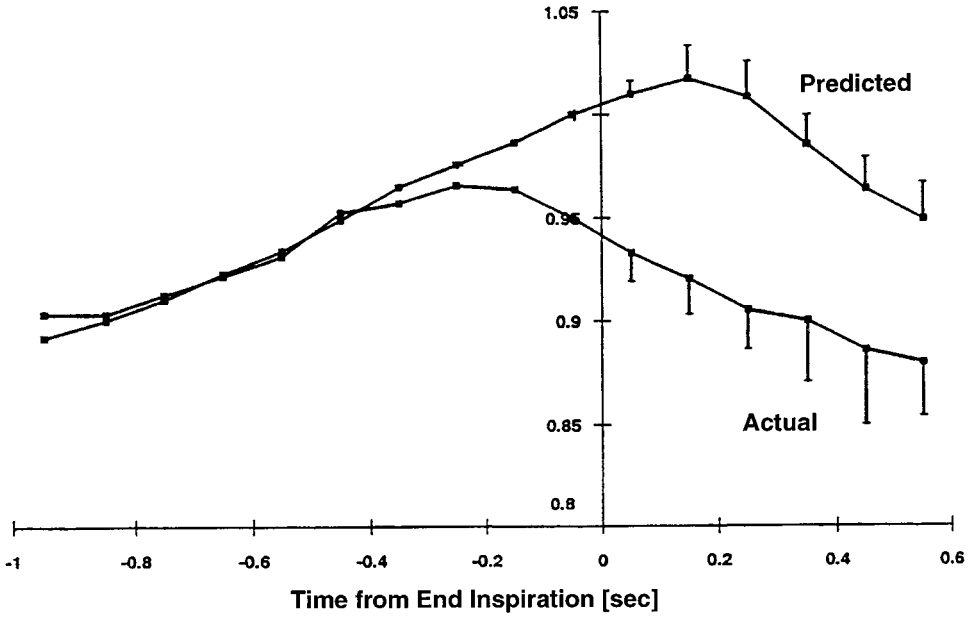

Fig. 5. Profile of group crural EMG Fc. *y*-Axis shows Fc, normalized to predicted end-inspiratory value of Fc for each subject. *x*-Axis scale shows time from end inspiration, as in Fig. 4. *Bottom* solid line and solid squares mark actual Fc values over each 100-ms period for the group. *Top* solid line and solid squares mark average Fc value over each 100 ms, predicted from inspiratory length-Fc relationship. Vertical bars, SE. Because length-Fc relationship was derived during inspiration, actual and predicted values converge. During postinspiration, actual values of Fc were significantly greater than predicted from inspiration.

consistent with earlier chronically implanted canines (7), in which we observed that mean moving average costal EMG was contained within the inspiratory flow envelope, whereas the profile of crural moving average EMG extended beyond the termination of inspiratory airflow well into the following expiration. Because the animals in this study were not tracheotomized, and these timing calculations were based on raw EMG sampled at 4 kHz, we believe these latest calculations of crural vs. costal PIIA to be more precise.

Experimental evidence about diaphragm PIIA is limited. There has been clear demonstration of diaphragm PIIA during resting breathing, without anesthetic, in humans (4, 20), cats (11), horses (15), and dogs (9, 10, 27). Diaphragm PIIA has been shown during anesthetic, although there is evidence, at least in crural diaphragm, that anesthetic significantly decreases the duration of PIIA (10). In one report (27), the duration of costal and crural PIIA was measured in awake, chronically implanted canines in the standing posture and was found to be roughly equal at ~8–9% of T_E. Clearly, that result is quite different from our findings here or from our prior reports (7–9).

Although we cannot easily reconcile the differing results about the duration of PIIA, it is important to note that our prominent crural PIIA measurements occurred in the right lateral decubitus position, whereas the lesser crural PIIA was described in standing animals (27). It would not be a surprise if posture altered PIIA; certainly, vagotomy and chemical stimulation, especially hypoxia, significantly change the presence of diaphragm PIIA (9, 13, 22, 27). That is, postinspiratory activity may originate centrally with highly specific late inspiratory and postinspiratory neurons in the ventral medulla (2, 3, 23), but its peripheral expression is subject to mechanical, chemical, and reflexic adjustment. We believe that it is important that no experimental report has ever claimed a significant or dominant role for costal diaphragm PIIA during resting breathing. Because the costal diaphragm is nearly bereft of spindles (or at least is much less populated with the end organs), the costal diaphragm would seem to be ill suited for a major role in muscle braking or controlled relaxation. By contrast, the crural diaphragm should be capable of fine dynamic adjustment of muscle length, affecting both costal and crural resting length as the two segments function together mechanically in series (17).

Crural Fc during PIIA. Moving beyond simple magnitude or duration of PIIA, can we gain some insight into diaphragm segmental function by examining the PIIA spectrum? We focused on crural PIIA of necessity because there was little costal PIIA to examine. The expectation that the character of crural PIIA EMG would not be simply a decrescendo mirror image of the inspiratory ramp has been expressed but not proven (4) and implied from central investigations of respiratory neurons (2, 3, 23).

Although we had available for study extensive crural EMG samples, it was not practical to simply examine crural EMG at a few identical, paired segmental lengths selected from inspiration and postinspiration. For some breaths the crural length through early inspiration was not absolutely identical to the range of length during PIIA, because crural diaphragm sometimes continued to shorten during postinspiration. Moreover, any type of spectral analysis is subject to large inherent variance (21), so a few paired Fc length observations per breath would have required a massive data set to reach any statistical conclusion regarding PIIA. Any attempt to compare Fc only at selected, matching lengths paired between inspiration and postinspiration would have wasted most of the EMG information available within each breath. To compare the two different phases of activation properly, it was necessary to take into account the range of muscle length through inspiration and postinspiration. This was accomplished simply by defining, through the early inspiratory ramp of EMG, a model of the relationship between the central tendency of the EMG spectrum (Fc) and the change in crural length, by linear regression. This crural Fc-length relationship, defined in inspiration, was then used to test Fc and length across the crural lengths in postinspiration. We reasoned that if postinspiration was simply a decreasing ramp, a mirror image of the increasing ramp of EMG in early inspiration, we would be able to correctly predict the Fc values in postinspiration. As shown in RESULTS, our predictions were not accurate; predicted postinspiratory values of Fc were significantly greater than those we actually measured. Evidently, the activation of crural diaphragm in inspiration and postinspiration, as evidenced by Fc of the EMG spectrum, was different.

At least two attributes of this analysis were important to ensure robust calculation. The first was that this technique allowed averaging over typically 20–30 breaths in each animal. This was important in controlling the large variance that is inevitable in all such fast Fourier transform estimates of EMG Fc. Second, this computation avoided any concern that changing muscle length might affect the EMG bipolar electrode and confound the measurement of EMG. In theory, changing interelectrode distance of bipolar EMG electrodes can influence the distribution of the EMG spectrum because of the frequency-selective filtering properties of this electrode configuration (16, 26). We avoided that potential problem. By comparing EMG spectra in the two opposite phases of inspiration at equivalent muscle length, the changes in Fc we observed reflected differences in muscle activation and not artifact arising from alterations in electrode geometry.

We must be circumspect in our interpretation of this observed difference in activation of crural diaphragm during inspiration and PIIA. The interpretation we prefer is that the decrease in crural Fc during PIIA reflects a change in recruitment of motor units in the latter portion of inspiration. This is a very appealing hypothesis, in keeping with current understanding that several distinctive types of respiratory neurons are fired in some combined sequence through the course of each breath (2, 3, 23). Intuitively, a different

pattern of muscle recruitment has mechanical appeal as well, because diaphragm braking could enlist motor units more suited to controlled relaxation, with a preponderance of fiber types that were perhaps slower and less fatigable. Unfortunately, this attractive interpretation remains speculative because there is a more mundane explanation for the fall in Fc during PIIA. The same motor units that were active during inspiration may simply have continued their activity in postinspiration, after a momentary pause, with firing rates slowing through PIIA as reflected in the fall in Fc at equivalent muscle length. Further study is required.

Influence of expiratory muscles. In this study, we treated EMG Fc as the "dependent" variable, which was predicted by crural length. Because that relationship failed to accurately predict Fc in PIIA, then apparently length was not sufficient explanation for the PIIA Fc. Alternatively, this could be interpreted to mean that the length of the diaphragm is not strictly related to EMG activity. That implication can be stated somewhat differently. Our results suggest that crural length is not dependent exclusively on EMG during postinspiration (assuming the regression relationship established during inspiration is valid). However, the opposite may be correct. Perhaps postinspiratory length is tightly related to EMG, but it is the early inspiratory length that is not well explained by EMG activity measured in early inspiration. The latter is more probable and could be caused by expiratory activity and/or recoil, which would mostly affect length in early inspiration rather than postinspiration.

By this reasoning, the length-Fc relationship in early inspiration should probably underestimate the Fc per length seen in postinspiration, because factors other than EMG are contributing to length change in early inspiration. However, this is not supported by our results because the length-Fc relationship derived in inspiration overestimated Fc for a given length in postinspiration.

Perhaps this discrepancy can be resolved by considering expiratory muscle activity that might affect crural length. We know from studies in other canines that in the right lateral decubitus position there is very little activity of the abdominal expiratory muscles, but the triangularis sterni may be an important influence (5). If rib cage expiratory muscle activity ceased abruptly at end expiration, the crural diaphragm might face an expansive rib cage recoil in early inspiration. Therefore, additional crural EMG activity might be required to develop diaphragm shortening in early inspiration compared with postinspiration. This could account for the greater than expected EMG activity in early inspiration, as noted in the previous paragraph.

Experimental assistance and animal care were provided by L. Jacques. The provision of all suture materials by Ethicon Sutures Ltd., a Johnson & Johnson Company, is gratefully acknowledged.

This work was supported by grants from the Medical Research Council of Canada and the Alberta Heritage Foundation for Medical Research. P. A. Easton was a Scholar of the Medical Research Council of Canada. R. S. Platt is a Student of the Alberta Heritage Foundation for Medical Research.

Present address of M. Katagiri: School of Allied Health, Kitasato University, 1-15-1 Kitasato, Sagamihara, 228 Kanagawa, Japan.

Address for reprint requests and other correspondence: P. Easton, Rm. 223, Heritage Bldg., University of Calgary, 3330 Hospital Dr. NW, Calgary, AB, Canada T2N 4N1.

Received 24 February 1998; accepted in final form 23 March 1999.

REFERENCES

1. **Aldrich, T. K., J. M. Adams, N. S. Arora, and D. F. Rochester.** Power spectral analysis of the diaphragmatic electromyogram. *J. Appl. Physiol*. 54: 1579–1584, 1983.
2. **Ballantyne, D., and D. W. Richter.** Post-synaptic inhibition of bulbar inspiratory neurons in the cat. *J. Physiol. (Lond.)* 348: 67–87, 1984.
3. **Ballantyne, D., and D. W. Richter.** The non-uniform character of expiratory synaptic activity in expiratory bulbospinal neurones of the cat. *J. Physiol. (Lond.)* 370: 433–456, 1986.
4. **Citterio, G., and E. Agostoni.** Discontinuity between inspiratory and posinspiratory diaphragm activity in man and rabbit. *Respir. Physiol*. 64: 295–306, 1986.
5. **De Troyer, A., and V. Ninane.** Triangularis sterni: a primary muscle of breathing in the dog. *J. Appl. Physiol*. 60: 14–21, 1986.
6. **Duron, B., M. C. Jung-Caillol, and D. Marlot.** Myelinated nerve fiber supply and muscle spindles in the respiratory muscles of cat: quantitative study. *Anat. Embryol. (Berl.)* 152: 171–192, 1978.
7. **Easton, P. A., T. Abe, J. Smith, J. W. Fitting, A. Guerraty, and A. E. Grassino.** Activity of costal and crural diaphragm during progressive hypoxia or hypercapnia. *J. Appl. Physiol*. 78: 1985–1992, 1995.
8. **Easton, P. A., J. W. Fitting, R. Arnoux, A. Guerraty, and A. E. Grassino.** Recovery of diaphragm function after laparotomy and chronic sonomicrometer implantation. *J. Appl. Physiol*. 66: 613–621, 1989.
9. **Easton, P. A., J. W. Fitting, R. Arnoux, A. Guerraty, and A. E. Grassino.** Costal and crural diaphragm function during CO_2 rebreathing in awake dogs. *J. Appl. Physiol*. 74: 1406–1418, 1993.
10. **Fitting, J. W., P. A. Easton, R. Arnoux, A. Guerraty, and A. Grassino.** Effect of anesthesia on canine diaphragm length. *Anesthesiology* 66: 531–536, 1987.
11. **Gauthier, H., J. E. Remmers, and D. Bartlett.** Control of the duration of expiration. *Respir. Physiol*. 18: 205–221, 1973.
12. **Gordon, D. C., C. G. M. Hammond, J. T. Fisher, and F. J. R. Richmond.** Muscle-fiber architecture, innervation, and histochemistry in the diaphragm of the cat. *J. Morphol*. 201: 131–143, 1989.
13. **Haxhiu, A. M., N. S. Cherniack, M. D. Altose, and S. G. Kelsen.** Effect of respiratory loading on the relationship between occlusion pressure and diaphragm EMG during hypoxia and hypercapnia. *Am. Rev. Respir. Dis*. 127: 185–188, 1983.
14. **Katagiri, M., R. Y. Young, R. S. Platt, T. M. Kieser, and P. A. Easton.** Respiratory muscle compensation for unilateral or bilateral hemidiaphragm paralysis in awake canines. *J. Appl. Physiol*. 77: 1972–1982, 1994.
15. **Kotera, A. M., P. C. Kosch, J. Beech, and T. Whitlock.** Breathing strategy of the adult horse (*Equus caballus*) at rest. *J. Appl. Physiol*. 64: 337–346, 1988.
16. **Lindstrom, L. H., and R. I. Magnusson.** Interpretation of myoelectric power spectra: a model and its applications. *Proc. IEEE* 65: 653–662, 1977.
17. **Macklem, P. T., and A. De Troyer.** A model of respiratory muscle mechanics. *J. Appl. Physiol*. 55: 547–557, 1983.
18. **Muller, N., G. Volgyesi, L. Becker, M. H. Bryan, and A. C. Bryan.** Diaphragmatic muscle tone. *J. Appl. Physiol*. 47: 279–284, 1979.
19. **Oppenheim, A. V., and R. W. Schafer.** *Digital Signal Processing*. Englewood Cliffs, NJ: Prentice-Hall, 1975, p. 195–283.
20. **Petit, J. M., G. Milic-Emili, and L. Delhez.** Role of the diaphragm in breathing in conscious normal man: an electromyographic study. *J. Appl. Physiol*. 15: 1101–1106, 1960.

21. **Platt, R. S., E. A. Hajduk, M. Hulliger, and P. A. Easton.** A modified Bessel filter for amplitude demodulation of respiratory electromyogram. *J. Appl. Physiol*. 84: 378–388, 1998.
22. **Remmers, J. E., and D. Bartlett.** Reflex control of expiratory airflow and duration. *J. Appl. Physiol*. 42: 80–87, 1977.
23. **Remmers, J. E., D. W. Richter, D. Ballantyne, C. Bainton, and J. Klein.** Reflex prolongation of stage I of expiration. *Pflügers Arch*. 407: 190–198, 1986.
24. **Richter, D. W.** Generation and maintenance of the respiratory rhythm. *J. Exp. Biol*. 100: 93–107, 1982.
25. **SAS Institute.** *SAS/Stat Guide for Personal Computers. Version 6*, edited by S. P. Joyner. Cary, NC: SAS Institute, 1985.
26. **Sinderby, C. A., A. S. Comtois, R. G. Thomson, and A. E. Grassion.** Influence of the bipolar electrode transfer function on the electromyogram power spectrum. *Muscle Nerve* 19: 290–301, 1996.
27. **Smith, C. A., D. A. Ainsworth, K. S. Henderson, and J. A. Dempsey.** Differential timing of respiratory muscles in response to chemical stimuli in awake dogs. *J. Appl. Physiol*. 66: 392–399, 1989.